

Nuclear Countermeasure Activity of TP508 Linked to Restoration of Endothelial Function and Acceleration of DNA Repair

Barbara Olszewska-Pazdrak,^{a,1} Scott D. McVicar,^a Kempaiah Rayavara,^b Stephanie M. Moya,^a Carla Kantara,^{a,b} Chris Gammarano,^a Paulina Olszewska,^a Gerald M. Fuller,^b Laurie E. Sower^b and Darrell H. Carney^{a,b,2}

^a Department of Biochemistry and Molecular Biology, The University of Texas Medical Branch, Galveston, Texas and ^b Chrysalis BioTherapeutics, Inc., Galveston, Texas

Olszewska-Pazdrak, B., McVicar, S. D., Rayavara, K., Moya, S. M., Kantara, C., Gammarano, C., Olszewska, P., Fuller, G. M., Sower, L. E. and Carney, D. H. Nuclear Countermeasure Activity of TP508 Linked to Restoration of Endothelial Function and Acceleration of DNA Repair. *Radiat. Res.* 186, 162–174 (2016).

There is increasing evidence that radiation-induced damage to endothelial cells and loss of endothelial function may contribute to both acute radiation syndromes and long-term effects of whole-body nuclear irradiation. Therefore, several drugs are being developed to mitigate the effects of nuclear radiation, most of these drugs will target and protect or regenerate leukocytes and platelets. Our laboratory has demonstrated that TP508, a 23-amino acid thrombin peptide, activates endothelial cells and stem cells to revascularize and regenerate tissues. We now show that TP508 can mitigate radiation-induced damage to endothelial cells *in vitro* and *in vivo*. Our *in vitro* results demonstrate that human endothelial cells irradiation attenuates nitric oxide (NO) signaling, disrupts tube formation and induces DNA double-strand breaks (DSB). TP508 treatment reverses radiation effects on NO signaling, restores tube formation and accelerates the repair of radiation-induced DSB. The radiation-mitigating effects of TP508 on endothelial cells were also seen in CD-1 mice where systemic injection of TP508 stimulated endothelial cell sprouting from aortic explants after 8 Gy irradiation. Systemic doses of TP508 that mitigated radiation-induced endothelial cell damage, also significantly increased survival of CD-1 mice when injected 24 h after 8.5 Gy exposure. These data suggest that increased survival observed with TP508 treatment may be due to its effects on vascular and microvascular endothelial cells. Our study supports the usage of a regenerative drug such as TP508 to activate endothelial cells as a countermeasure for mitigating the effects of nuclear radiation. © 2016 by Radiation Research Society

INTRODUCTION

With the increasing probability of nuclear accidents or detonation of a nuclear device, it is important that medical countermeasures be developed to mitigate effects of radiation exposure. Estimates suggest that thousands of people could die from a small nuclear detonation in any major city. Most deaths would occur from acute radiation syndrome (ARS), caused by high doses of radiation, although a large number of individuals are also likely to die after exposure to lower doses of radiation combined with traumatic injuries and burns [collectively referred to as radiation combined injury (RCI)] (1, 2), or from delayed radiation effects that manifest months later (3, 4). Current therapeutic drug approaches have focused on reversing radiation-induced effects by maintaining the normal levels of leucocytes and platelets or maintaining intestinal crypts (5). These treatments include scavengers of reactive oxygen species (ROS), anti-apoptotic drugs, drugs that accelerate DNA repair and those that target specific inflammatory signaling pathways (5). Although a number of these drugs enhance early survival (5), they typically do not address RCI or delayed radiation-induced effects. This has prompted a re-evaluation of radiation-induced effects on endothelial cells and the potential of developing drugs to reverse radiation-induced effects on microvascular endothelial cells in capillary networks that contribute to acute and long-term radiation-induced damage to multiple tissues.

The vascular endothelium is one of the largest organ systems in the body with trillions of cells that must be maintained to provide oxygen and nourishment to all body tissues. Recent studies indicate that endothelial function and nitric oxide (NO)-dependent vasodilation are compromised by low doses of radiation, often before any morphological effects can be observed (6–8). Moreover, radiation-induced damage may specifically affect survival and function of microvascular endothelial cells that supply stem cell niches in bone marrow, intestinal crypts and other tissues (4, 9–11).

Ionizing radiation causes endothelial dysfunction (ED) and loss of NO signaling in endothelial cells by increasing

¹ Author's current address: Department of Pathology, Baylor College of Medicine, One Baylor Plaza, Houston, TX 77030.

² Address for correspondence: Department of Biochemistry and Molecular Biology, The University of Texas Medical Branch, 301 University Blvd., Galveston, TX 77555-0645; email: dcarney@utmb.edu.

ROS, downregulating expression of endothelial nitric oxide synthase (eNOS) (12, 13) and by increasing levels of pro-inflammatory cytokines such as TNF- α and IL-6 (10, 14–18). Radiation-induced ED causes early apoptosis of endothelial cells in microvessels and intestinal arterioles (13, 19). ED is also known to promote inflammation, thrombosis and vascular leakage (20–22) and to reduce levels of thrombomodulin and activated protein C (23–26). These pathophysiological events contribute to progression toward sepsis, multiple organ failure and death (25, 27). Thus, by reversing radiation-induced ED it may be possible to increase survival, delay onset of acute mortality and prevent late effects of radiation.

We have previously shown that TP508 treatment of human endothelial cells upregulates and activates eNOS to reverse ED and produce NO (28). Moreover, this effect of TP508 reverses hypoxia-induced ED to restore VEGF responsiveness, NO signaling and aortic endothelial cell sprouting (29). TP508 has also been shown to restore vascular function and prevent ischemic damage in porcine models of chronic myocardial ischemia (30) and acute myocardial infarct (31, 32). These effects of TP508 suggested that it might mitigate radiation-induced effects on endothelial cells.

Our current study shows that, indeed, TP508 mitigates effects of nuclear radiation on human endothelial cells in culture restoring endothelial NO production, tube formation and accelerating repair of radiation-induced DNA double-strand breaks (DSB). We also show that TP508 systemic injection mitigates radiation-induced effects on endothelial cells *in vivo* and significantly increases the survival of mice exposed to lethal doses of nuclear radiation (8.5 Gy, LD₇₀).

MATERIALS AND METHODS

Reagents

Thrombin peptide TP508 (AGYKPDEGKRGDACEGDSGGPFV, rusalatide acetate, CAS no. 87455-82-6) was synthesized and purified by American Peptide Company (now Bachem Americas Inc., Sunnyvale, CA). Matrigel™ matrix (growth factor reduced, phenol red free) was obtained from BD Biosciences (Bedford, MA). Sterile 0.9% saline for injection was obtained from Hospira (Lake Forest, IL). L-arginine and all other reagents were purchased from Sigma-Aldrich® LLC (St. Louis, MO) unless otherwise noted.

Endothelial Cells

Primary human coronary artery endothelial cells (HCAEC) purchased from Lonza, Inc. (Walkersville, MD) were cultured in endothelial cell basal media (EBM) supplemented with 5% fetal bovine serum (FBS) and SingleQuots™ growth factors (EGM; Lonza, Inc.) in 5% CO₂ at 37°C and used for assays between passages 4–8. Primary adult human dermal microvascular endothelial cells (HDMEC), purchased from PromoCell (Heidelberg, Germany), were cultured in EBM supplemented with serum and endothelial cell growth factors (EGM2-MV; PromoCell) in 5% CO₂ at 37°C and used for assays between passages 4–8. Pericytes isolated from placenta (PromoCell) were cultured in pericyte growth media (PromoCell) in 5% CO₂ at 37°C and used for assays between passages 3–9.

Nitric Oxide Assay

Two-day post-confluent cultures of HCAEC in 24-well plates were sham or 8 Gy irradiated using a cesium-137 (¹³⁷Cs) gamma irradiator (Mark 30; JL Shepherd, San Fernando, CA). After 24 h, media was replaced with EBM containing 200 μ M L-arginine (250 μ l/well) and cells were treated with TP508 (50 μ g/ml) or VEGF (50 ng/ml). These doses were selected based on optimal NO responses in HCAEC (28). Supernatants were collected and analyzed for NO concentration using a chemiluminescence NO analyzer (model no. 270B; Sievers Instruments, Boulder, CO) as previously described (28, 30). The analyzer was calibrated for each experiment using a sodium nitrite standard curve. Nitric oxide concentration in the EBM containing L-arginine was used as a background value and was subtracted from sample values to determine the amount of NO released from cells. To determine whether TP508 could mitigate effects of radiation on NO production, sham- and 8 Gy irradiated endothelial cells were treated with TP508 (50 μ g/ml) or saline (vehicle control) at 1 h postirradiation, and NO production was determined at 18 h postirradiation, as described above.

Western Blot Analysis

Human coronary artery endothelial cells were grown in 12-well tissue culture plates and either sham or 8 Gy gamma irradiated at 1 h postirradiation, the sham- and 8 Gy irradiated cells were treated with saline alone or TP508 (50 μ g/ml). After 24 h the media was removed, cells were washed once with PBS and lysed using lysis buffer (150 mM NaCl; 50 mM HEPES, pH 7.4; 1 mM EGTA; 1 mM Na₃VO₄; 10 mM NaF; 1 mM phenylmethylsulfonyl fluoride; 5% glycerol; and 1% Triton™ X-100) containing a protease inhibitor mixture (Roche Diagnostics, Indianapolis, IN). Cell lysates were solubilized, separated on SDS-PAGE and transferred to nitrocellulose (Invitrogen™, Grand Island, NY). Nitrocellulose membranes were incubated overnight at 4°C with primary antibodies against phospho-eNOS (S1177) and GAPDH as a loading control (Santa Cruz Biotechnology®, Santa Cruz, CA) as described previously (28). Immunoblots were developed using Immobilon™ Western Detection Reagents (EMD Millipore, Billerica, MA).

Tube Formation Assays

Confluent cultures of HDMEC and pericytes were irradiated (3 Gy) using a ¹³⁷Cs gamma irradiator. Cells were harvested 1 h later and combined at a ratio of 1:100 pericytes:HDMEC. Cells were pelleted at 500g for 5 min, the supernatant was then removed and the pellet was resuspended in EBM containing either 10 μ g/ml TP508 with saline or saline alone. Cells were then incubated on Matrigel in 15-well iBidi® Angiogenesis μ -Slides (Planegg, Germany) for 24 h in 5% CO₂ at 37°C. Wells were analyzed at various time points using phase contrast microscopy on a Leica DMLB microscope (Buffalo Grove, IL) and images were captured using a Moticam Pro 285D CCD camera with Motic Live imaging software (Xiamen, China). Mean total tube formation length per well was determined using ImagePro® 7.0 (Media Cybernetics Inc., Rockville, MD).

Analysis of DNA Repair

Glass coverslips placed in 24-well tissue culture plates were seeded with 25,000 HDMEC in 0.5 ml EGM2-MV media per well and incubated overnight at 37°C, 5% CO₂. The following day, 1 h postirradiation, media was removed and replaced with EGM2-MV media supplemented with 2% (v/v) sterile saline or TP508 and sterile saline (final concentration 200 μ g/ml of media). HDMEC were either 3 or 6 Gy irradiated using a ¹³⁷Cs gamma irradiator, then returned to the incubator.

Analysis of DNA DSB was performed by immunofluorescent visualization of phosphorylated histone 2AX (γ -H2AX) binding to

DSB within the nuclei. At each time point after irradiation, media was removed, and coverslip cultures were rinsed with Dulbecco's phosphate buffered saline (DPBS), then fixed with 4% formalin for 30 min at room temperature. Cells were permeabilized for 1 h with 0.2% Triton X-100 in DPBS, then blocked overnight with 10% goat serum. Cells were then incubated with 1:1,000 mouse anti-human γ -H2AX (Ser136) antibody (cat. no. 05-636; EMD Millipore) followed by incubation with 1:500 goat anti-mouse Alexa Fluor® 488 conjugated secondary antibody (cat. no. A-11001; Life Technologies, Grand Island, NY). Cell nuclei were counterstained with 300 nM DAPI. Coverslips were then inverted and mounted onto glass slides with ProLong® Gold mounting media.

Fluorescence microscopy was performed using a Leica DMLB microscope with EL6000 external fluorescence light source with filter cubes for DAPI and Alexa 488 secondary antibody. Eight random fields per coverslip (4× objective) were imaged to ensure counting of γ -H2AX-labeled foci within at least 100 distinct nuclei. Images were automatically analyzed with CellProfiler version 2.1.1 (33) to determine the number of γ -H2AX-labeled foci within each nucleus, as well as the number of nuclei that contained no foci, indicative of DSB repair. Data were exported to GraphPad Prism version 6.05 (La Jolla, CA), for statistical analysis. Mean and 95% confidence intervals were generated using descriptive statistical analysis of the histograms of repeated measures for each treatment and time point. *P* values adjusted for the multiple comparisons between groups were generated using the Kruskal-Wallis one-way analysis of variance (ANOVA) nonparametric test to account for differences in the number of nuclei counted.

Animals and Animal Experiments

All experiments were conducted at the University of Texas Medical Branch (UTMB) using an IACUC-approved protocol. CD-1 outbred 12–15-week old male mice [(ICR) Harlan® Laboratories, Houston, TX] were housed, five per cage, in a controlled environment with a 12:12 h light-dark schedule, temperature of $21 \pm 0.5^\circ\text{C}$ and room humidity of $50\% \pm 20\%$ within the Animal Research Center at UTMB. Water and chow were provided *ad libitum*. Mice were allowed to acclimate for at least seven days prior to initiation of experiments.

Irradiation. The mice were anesthetized using isoflurane and individually placed into a pie cage (10 mice/cage). To ensure uniform exposure of the animals, the pie cage was set on a turntable that rotated at a rate of 5 rpm inside the ^{137}Cs gamma irradiator chamber. The mice received 3–10 Gy at a dose rate of 458 cGy/min whole-body gamma irradiation. Landauer® nanoDot™ OSLD dosimeters (Glenwood, IL) were placed at three locations within each pie cage (inner, middle and outer) to verify radiation dose exposures. There was less than or equal to 4.3% coefficient of variation at each position between experiments. The middle position standard deviation was 0.2 Gy.

Mouse aortic explant angiogenesis assay. One hour after irradiation, mice were placed in a restrainer and intravenously (i.v.) injected through the tail vein with a single dose of TP508 in 100 μl sterile saline or 100 μl sterile saline alone. After 24 h, the mice were euthanized by CO_2 inhalation and thoracic aortas were isolated from TP508- or saline-alone treated mice and transferred to culture dishes containing cold sterile EBM, as previously described (34, 35) The periaortic fibro-adipose tissue was removed under a dissecting microscope and aortas were rinsed with cold EBM and cut transversely to create 1 mm aortic rings (~10 per aorta). Aortic rings were cut, opened, and the inner endothelial surface was placed directly on Matrigel matrix-coated 24-well plates. Aortic explants were cultured in a 5% CO_2 atmosphere at 37°C in EGM containing 5% FBS and SingleQuots endothelial growth factors (Lonza, Inc.). Endothelial cell sprouting was monitored daily by inverted phase contrast microscopy (Nikon® Instruments Inc., Melville, NY) and images were captured using SPOT RT camera and advanced imaging software (Sterling Heights, MI) at 40× and 100× magnification.

Image analysis and quantification for area occupied by sprouting endothelial cells and maximal endothelial cell migration from aortic explants edges were performed using MetaMorph® software (Molecular Devices, Downingtown, PA). For each experiment, aortas were isolated from three saline-alone and three TP508-treated mice. Aortic sprouting was quantified from triplicate culture wells containing a total of six aortic explants per experimental condition. Area of endothelial sprouting was normalized to the perimeter of aortic explants visualized in the field of observation. Area of sprouting from saline-alone treated mouse explants cultured for five days was expressed as a value of 1.0. For maximum endothelial cell migration, the longest distance of migrated cells from the edges of aortic explants was measured in three different regions from each explant. ANOVA was used to determine if there was a significant difference among groups. A pair-wise comparison of groups was then done using the Tukey's test. A *P* value of <0.05 was regarded as significant.

Thirty-day survival analysis. CD-1 12-week-old male mice were whole-body gamma-irradiated (8.5 Gy, LD_{70}) using a ^{137}Cs gamma irradiator. At 24 h postirradiation, mice were injected subcutaneously (sc) with a single 100 μl dose of sterile saline alone or with TP508 in saline (350 μg ; 10 mg/kg; 20 mice per group). Mice were monitored twice daily for up to 30 days. Mice were euthanized based on a pain assessment scoring system consistent with our UTMB IACUC-approved protocol or at the veterinarian's discretion. Euthanasia of a mouse prior to day 30 was equated to a mortality event, whereas, mice sacrificed at the end of the study were considered to have survived. The data were analyzed using Kaplan-Meier-based GraphPad analysis. Statistical significance was defined as $P < 0.05$. *P* values were calculated using the Gehan-Breslow-Wilcoxon test and confirmed using the Log-rank (Mantel-Cox) test.

RESULTS

In Vitro Effects of TP508 on Radiation-Induced Endothelial Dysfunction

Our previous studies showed that TP508 stimulates eNOS to produce NO (28) and reverses effects of hypoxia-induced ED to restore myocardial function (30) and prevent the loss of endothelial cell responses to VEGF (29). Because exposure to radiation has been shown to induce ED (6–8, 12, 13), we conducted studies to determine whether irradiation of HCAEC would affect NO production by endothelial cells in response to VEGF or TP508, which stimulate NO production by two different mechanisms (28).

We show in Fig. 1A, VEGF treatment of sham-irradiated HCAEC stimulated a fivefold increase in NO production. In the same sham-irradiated cells, TP508 treatment caused a ninefold increase in NO production. Irradiation (8 Gy) of HCAEC caused a complete loss of VEGF-stimulated NO production over sham-irradiated HCAEC when measured 24 h postirradiation (Fig. 1A). In contrast, when 8 Gy irradiated cells were TP508 treated, NO production was still significantly stimulated (>sixfold) at 24 h postirradiation. Thus, TP508 treatment was able to stimulate NO production in the irradiated cells, while VEGF treatment did not stimulate NO production.

We then investigated whether TP508 treatment of cells 1 h postirradiation could prevent or diminish radiation-induced attenuation of NO production in response to VEGF or TP508. As shown in Fig. 1A, when cells were treated with TP508 1 h postirradiation (8 Gy), VEGF stimulation of

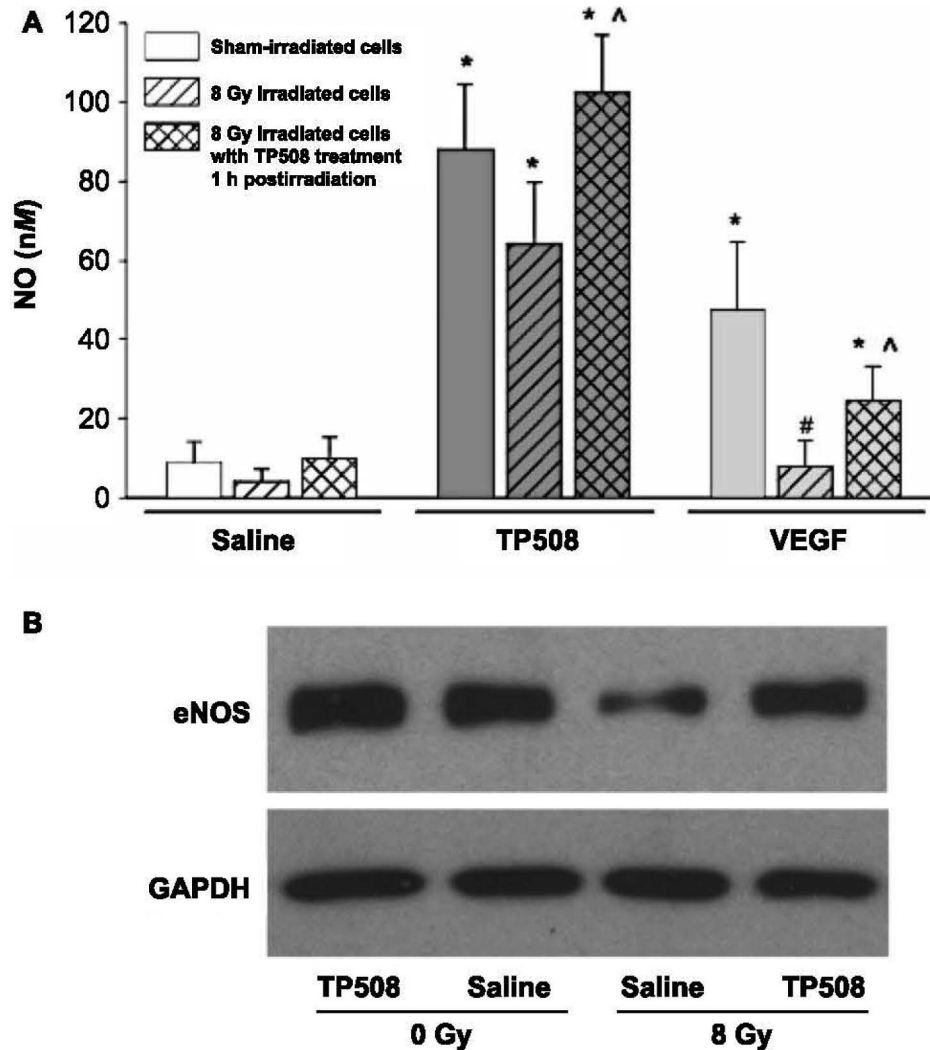


FIG. 1. Effect of 8 Gy irradiation on NO production in response to TP508 and VEGF. Panel A: Two-day post-confluent cultures of HCAEC were sham-irradiated (solid bars) or 8 Gy gamma irradiated (hatched bars). After 24 h, media was replaced with EBm containing 200 μ M L-arginine and cells were treated for 1 h with saline (vehicle; white bars), TP508 (50 μ g/ml; dark gray bars) or VEGF (50 ng/ml; light gray bars). Supernatants were collected and analyzed for NO, as described in Materials and Methods. To determine if TP508 could mitigate effects of radiation, HCAEC were treated 1 h postirradiation with TP508 (50 μ g/ml; cross-hatched bars) and then assayed for NO production 24 h later, as described above. * P < 0.01 vs. saline alone; # P < 0.01 vs. VEGF-treated; and ^ P < 0.05 vs. 8 Gy irradiated cells treated with VEGF without TP508. Panel B: Western blot analysis of eNOS expression from HCAEC 24 h after sham irradiation or 8 Gy irradiation and treated at 1 h postirradiation with saline (vehicle) or TP508 (50 μ g/ml; TP). Blot was reprobbed with GAPDH as protein loading control.

NO production measured at 24 h postirradiation was partially restored relative to saline-alone treated cells, resulting in a significant increase in NO production (2.8 fold over controls). Moreover, in these cells that were treated with TP508 1 h postirradiation, TP508 treatment 24 h later stimulated NO production by >ninefold, which was equivalent to the stimulation seen with TP508 treatment of sham-irradiated cells.

These results suggest that irradiation of HCAEC may have reduced eNOS expression or the activation of eNOS and that TP508 treatment 1 h postirradiation, mitigated or diminished this radiation-induced effect. Indeed, Western

blot analysis showed that there was approximately a 50% reduction of eNOS protein expression in endothelial cells 24 h postirradiation (8 Gy) (Fig. 1B). However, TP508 treatment 1 h postirradiation (8 Gy) prevented the radiation-induced downregulation of eNOS (Fig. 1B). These results suggest that TP508 treatment reversed radiation-induced ED and loss of NO signaling by attenuating the downregulation of eNOS expression.

TP508 Effects on Endothelial Tube Formation

To determine whether the radiation-induced decrease of endothelial NO signaling correlated with behavior of cells in

culture, we evaluated TP508 effects on endothelial tube formation using an established Matrigel tube formation assay (36). Co-cultures of pericytes with microvascular endothelial cells were used *in vitro* to closely mimic the *in vivo* microvascular environment (37, 38). Confluent cultures of HDMEC and human pericytes in separate flasks were gamma irradiated (3 Gy) or sham irradiated (0 Gy). Cells were harvested 1 h later and combined at a ratio of 1:100 pericytes:HDMEC, treated with 10 $\mu\text{g}/\text{ml}$ TP508 or saline alone and then plated (10,000 cells per well) onto Matrigel matrix. Sham-irradiated cells elongated and formed tube-like structures after 18 h (Fig. 2A). In contrast, cell elongation and tube formation in the gamma-irradiated cells were almost completely inhibited (Fig. 2C). Treating the co-cultured cells with TP508 1 h postirradiation, however, increased cell elongation and formation of tube-like interconnecting structures (Fig. 2D). Quantification of this data shows that 3 Gy irradiation resulted in more than a 70% reduction in tube formation (Fig. 2E), however, TP508 significantly increased tube formation in these cells, more than doubling the amount of tube formation seen in the 3 Gy irradiated saline-alone treated cells. These results indicate that TP508 treatment not only reduces radiation-induced inhibition of endothelial NO signaling, but also mitigates damaging effects of radiation that prevent functional tube formation.

TP508 Effect on Radiation-Induced DNA Damage

Ionizing radiation creates ROS inside of cells within seconds of exposure, resulting in DNA DSB which, if not repaired, contribute to radiation-induced senescence, apoptosis and cell death within tissues (39). Since, TP508 treatment mitigated radiation-induced loss of endothelial function, we wanted to determine if the protective effects of TP508 could also enhance repair of DNA DSB.

Within seconds of DSB formation, histone H2AX (an isoform of histone H2A) is phosphorylated at Ser139 by ataxia telangiectasia mutated (ATM) and other kinases to form γ -H2AX (40). This creates localized chromatin remodeling necessary to allow DNA repair proteins to assemble at the DSB site. Immunofluorescent labeling of γ -H2AX at the site of each DSB creates foci or “speckles” that can be visualized using fluorescent microscopy (Fig. 3A–D). In these experiments, cells were treated with TP508 or saline alone 1 h postirradiation, because the process of DNA repair begins very quickly after DSB formation and because we wanted to examine repair during the first hour postirradiation. To aid in visualization and quantification of DSB γ -H2AX foci, we utilized CellProfiler imaging software (33) to automate an analysis pipeline where DAPI fluorescent images are used to create a mask defining the extent of each nucleus, and then apply it to the corresponding images of Alexa Fluor 488-labeled γ -H2AX to determine the number of foci within each nucleus.

One hour after 3 Gy irradiation of HDMEC, the majority of cell nuclei exhibit 10–15 foci per nucleus (Fig. 3A, B and F) independent of treatment. By 5 h, however, HDMEC treated with TP508 (200 $\mu\text{g}/\text{ml}$) 1 h postirradiation showed a significantly reduced number of foci present in each nuclei compared to saline-alone treated cells (2.6 vs. 7.0, $P < 0.001$) (Fig. 3C, D and F). The number of cells that had fully repaired DSB and no foci by 5 h was also increased from 23% in saline-alone treated cells to 49% in TP508-treated cells. By 9 h postirradiation, 69% of the TP508-treated HDMEC were completely repaired, over twice as many as in the saline-alone treated group (32%; Fig. 3F).

After 6 Gy irradiation, increased DNA repair of HDMEC pretreated with 200 $\mu\text{g}/\text{ml}$ TP508 is even more evident. Doubling the ionizing radiation dose increased the mean number of foci counted at 1 h from approximately 14–23 speckles per nucleus (Fig. 4A, B and F). Rapid repair in HDMEC in the TP508 treatment group resulted in highly significant reductions in mean γ -H2AX foci per cell compared to the saline-alone treated group as early as 2.5 h postirradiation (11.4 vs. 19.4, $P < 0.0001$) (Fig. 4E). This trend continued at 5 (7.0 vs. 9.9, $P < 0.001$) and 9 h (2.1 vs. 6.0, $P < 0.0001$) postirradiation. Increasing the dose of ionizing radiation from 3 to 6 Gy also decreased the percentage of HDMEC with fully repaired DSB at 5 and 9 h (Fig. 4C–E). Only 8% of HDMEC were completely repaired by 5 h in the saline-alone treated samples, compared to 23% with TP508 treated samples. At 9 h, these values were 17 and 60%, respectively. Thus TP508 dramatically increased the number of HDMEC with completely repaired DSB after 6 Gy irradiation *in vitro*, effectively tripling the percentage of γ -H2AX foci-free cells at both the 5 and 9 h time points.

TP508 Effects on Endothelial Cells within Animals

We recently demonstrated that i.v. injection of TP508 stimulated aortic endothelial cell sprouting and prevented hypoxia-induced loss of endothelial function when aortic explants were removed from nonirradiated mice 24 h after injection and cultured on Matrigel *ex vivo* (29). Thus, we chose to use this modified aortic sprouting assay to determine whether systemic injection of TP508 could protect endothelial function *in vivo* after whole-body gamma irradiation.

CD-1 mice received 0, 3, 8 or 10 Gy whole-body irradiation (^{137}Cs gamma irradiator). Mice were injected through the tail vein 1 h postirradiation with 100 μl of saline alone or 100 μl of saline containing 500, 100 or 20 μg of TP508. Thoracic aortas were isolated 24 h later and aortic explants were cultured *ex vivo* on Matrigel-coated 24-well plates and cultured in EGM media containing endothelial cell growth factors as previously described (29).

As shown in Fig. 5, injection of TP508 (500 μg) in sham-irradiated animals significantly increased the amount of endothelial cell sprouting from aortic explants (Fig. 5A). As the dose of radiation increased, the amount of sprouting

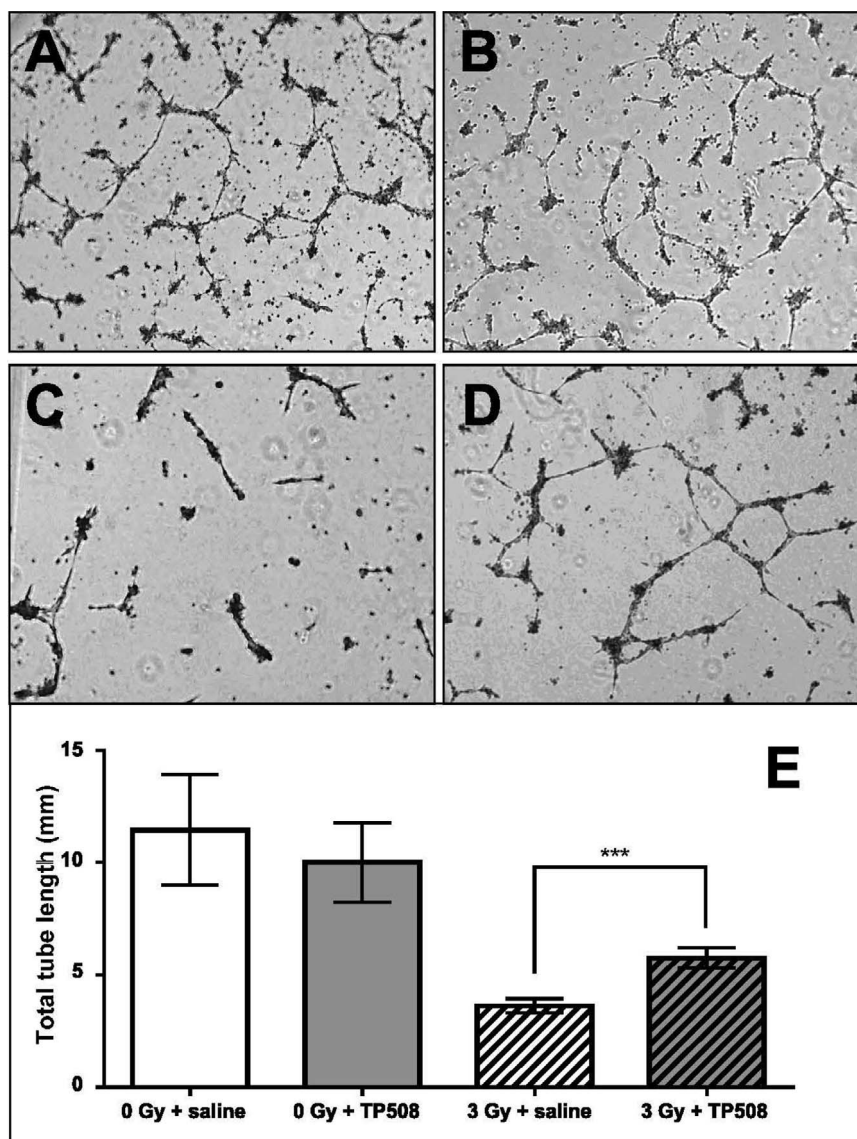


FIG. 2. Effect of radiation and TP508 on endothelial cell tube formation. Confluent cultures of HDMEC and human pericytes were 3 Gy irradiated with a ^{137}Cs gamma irradiator as described in Materials and Methods. Cells were harvested 1 h later and combined at a ratio of 1:100 pericytes:HDMEC, then resuspended in EBM containing either 10 $\mu\text{g}/\text{ml}$ TP508 or vehicle (0.9% saline). Co-cultures were then incubated on Matrigel for 24 h. Representative images show extent of tube-like networks at 18 h formed in nonirradiated saline-alone treated cells (panel A), nonirradiated TP508-treated cells (panel B), 3 Gy irradiated saline-treated cells (panel C) and 3 Gy irradiated TP508-treated cells (panel D). Mean total tube formation length per well (panel E) was determined using ImagePro 7.0. Total $n = 3-8$ wells; error bars = 95% CI; *** $P < 0.001$.

from explants decreased and was no longer visible in most aortic explants from animals exposed to 8 or 10 Gy. In contrast, explants from animals treated with TP508 1 h postirradiation continued to exhibit sprouting, even after 10 Gy irradiation (Fig. 5A). Quantification of the area of sprouting (Fig. 5B) or maximal length of sprouts (not shown) from six explants per group indicated that TP508 significantly increased the sprouting in sham-irradiated and irradiated animals, more than doubling the amount of sprouting in explants from animals at all exposure doses.

Quantification of the amount of sprouting stimulated by injection of various doses of TP508 showed a dose-

dependent effect *in vivo* (Fig. 6). Endothelial cell sprouting from aortic explants isolated from 3 Gy irradiated mice was significantly stimulated by all doses of TP508 with maximal stimulation at 100 μg , which was 55% over the amount of sprouting observed in sham-irradiated mice (Fig. 6A). In 8 Gy irradiated animals, TP508 treatment again significantly stimulated sprouting compared to 8 Gy irradiated, saline-alone treated animals (Fig. 6B). In these experiments the area of sprouting was less than that observed in explants from sham-irradiated animals, but there was a clear dose response with the 500 μg TP508 treatment producing the greatest amount of sprouting (Fig. 6B).

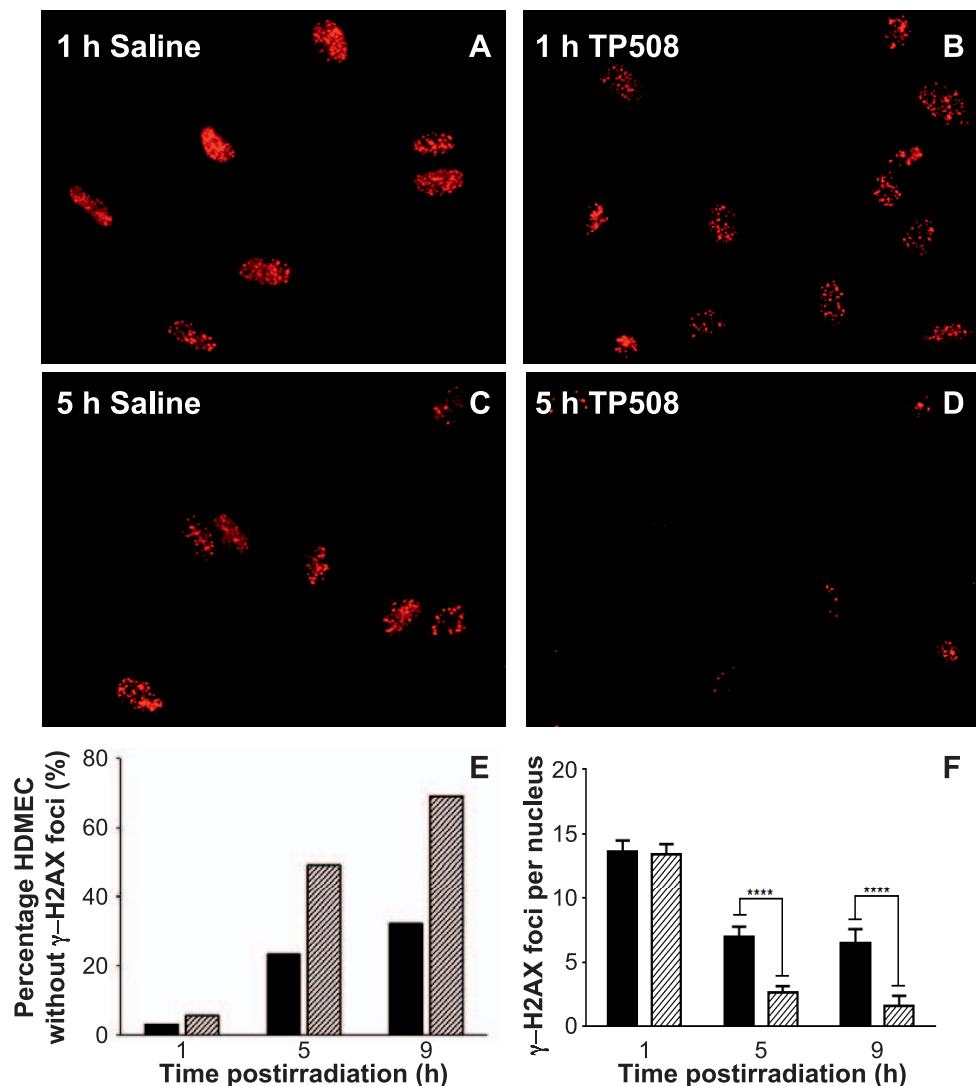


FIG. 3. Effect of TP508 on DNA repair in HDMEC after 3 Gy irradiation. HDMEC were treated with saline alone (panels A and C) or 200 μ g/ml TP508 (B and D) 1 h postirradiation with 3 Gy (see Materials and Methods). Cells were fixed in formaldehyde at 1, 5 and 9 h postirradiation and radiation-induced DNA DSB were visualized using immunofluorescent staining of γ -H2AX foci (red) (panels A and B, 1 h postirradiation; panels C and D, 5 h postirradiation). CellProfiler analysis of eight random fields for each condition and time point was used to determine the percentage of DAPI-stained nuclei in eight random fields with complete DNA repair (no foci) (panel E) and the number of foci per nucleus (panel F). Saline-treated controls (black); TP508 (200 μ g/ml) (hatched bars). Total $n = 180$ –240 nuclei counted per condition; error bars = 95% CI; **** $P < 0.0001$.

TP508 Effects on Survival

It has been suggested that acute radiation-induced mortality caused by gastrointestinal breakdown (GI-ARS) is linked to the early apoptosis of endothelial cells within the intestinal and colonic crypts that supply oxygen and nutrients to the crypt stem cells (9). Because of the significant protection of the endothelial cells observed in our study of TP508, both *in vitro* and by systemic injection into animals, we hypothesized that TP508 would increase animal survival if injected systemically. Additional studies, reported elsewhere, demonstrated that TP508 treatment up to 24 h postirradiation protected stem cells within

gastrointestinal crypts and maintained crypt integrity (41). Because it is expected that treatment of victims exposed to nuclear radiation may take at least 24 h, all of our survival studies have been conducted with 24 h postirradiation injections.

As shown in Fig. 7, a single injection of TP508 (10 mg/kg) given 24 h after 8.5 Gy gamma irradiation, significantly increased 30-day survival in mice, from 26.7 to 73.3% ($P < 0.01$) (Fig. 7A). This represents a 46.6% increase in total percentage survival, nearly tripling the number of animals that survive. These results demonstrate that TP508 may be an effective nuclear radiation countermeasure to increase survival after exposure.

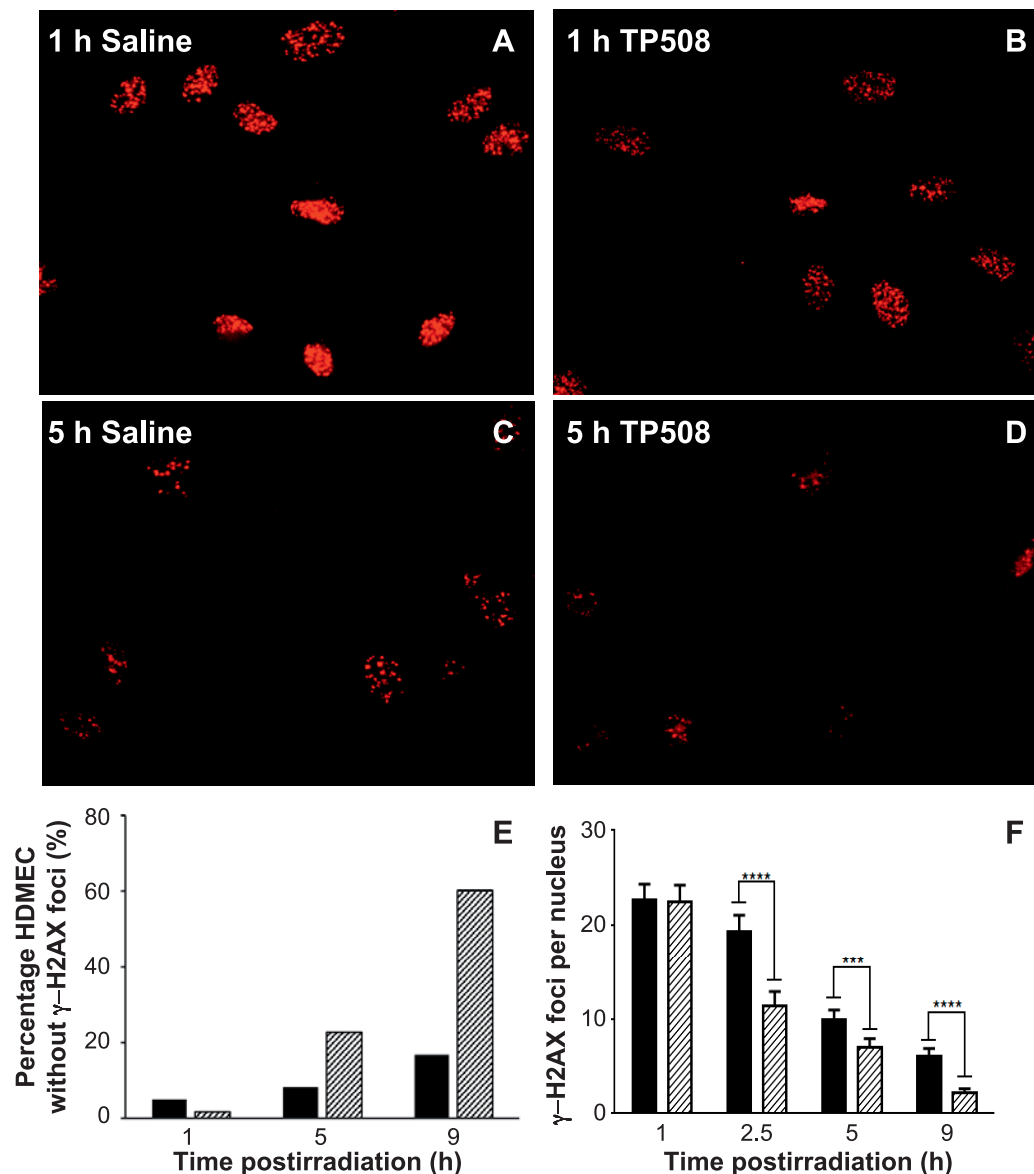


FIG. 4. Effect of TP508 on DNA repair in HDMEC after 6 Gy irradiation. HDMEC were treated with saline alone (panels A and C) or 200 μ g/ml TP508 (panels B and D) and 6 Gy gamma irradiated (Materials and Methods). Cells were fixed in formaldehyde at 1, 2.5, 5 and 9 h postirradiation and radiation-induced DNA DSB were visualized using immunofluorescent staining of γ -H2AX foci (red) (panels A and B, 1 h postirradiation; panels C and D, 5 h postirradiation). CellProfiler analysis of eight random fields for each condition and time point were used to determine the percentage of DAPI-stained nuclei in eight random fields with complete DNA repair (no foci) (panel E) and the number of foci per nucleus (panel F). Saline-alone treated (black); TP508 (200 μ g/ml) (hatched bars hash). Total n = 180 to 240 nuclei counted per condition; Error bars = 95% CI; *** P < 0.001, **** P < 0.0001.

DISCUSSION

The vascular endothelium is one of the largest organ systems in the body with trillions of cells that must be maintained to provide oxygen and nourishment to all body tissues. It is now established that even low doses of radiation cause loss of endothelial function and reduced NO signaling, often before any morphological effects can be observed (6–8, 42). It follows that radiation likely affects survival and function of microvascular endothelial cells that supply stem cell niches in bone marrow, intestinal crypts

and other tissues (4, 9–11). *In vivo* studies have shown that microvascular endothelial cell apoptosis begins from 1 to 24 h postirradiation (9, 43) and capillaries begin to disintegrate as early as 1 day postirradiation (44). Effects of radiation-induced endothelial cell damage are also associated with long-term radiation-induced effects in brain (6, 43), lung (45, 46) and myocardial disease (42, 47). Thus, preventing radiation-induced endothelial cell apoptosis and restoring endothelial cell NO signaling may mitigate acute radiation-induced mortality and prevent delayed effects of radiation that manifest months later.

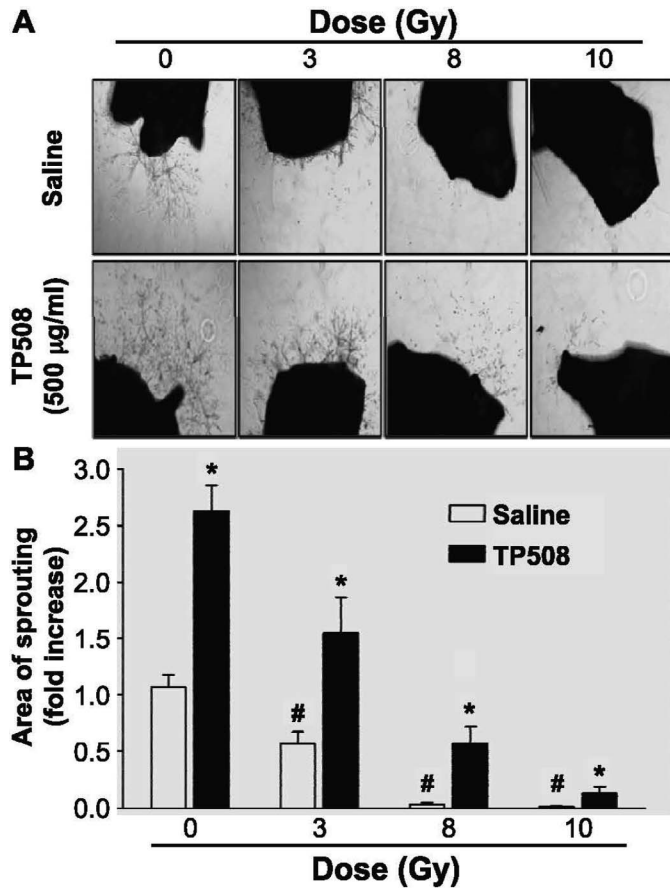


FIG. 5. Effect of radiation and TP508 on endothelial cell sprouting from aortic explants. Thoracic aortas were isolated 24 h after sham irradiation and 3–10 Gy irradiation of CD-1 mice that were i.v. injected (tail vein) 1 h postirradiation with saline-alone (open bars) or TP508 (500 µg/ml; black bars). Aortic explants were cultured on Matrigel for 5 days. Panel A: Digital images are representative of the best sprouting from 8 to 10 explants per group. Panel B: Bar graph shows quantification of area of endothelial sprouting (8–10 explants per group). Data are presented as mean \pm SD. * P < 0.05 compared to saline at each radiation dose; # P < 0.05 compared to saline with sham irradiation.

Extensive studies from our laboratory have shown that the thrombin-derived TP508 peptide targets endothelial cells and activates eNOS to produce NO (28). This peptide drug reversed hypoxia-induced ED to restore VEGF-stimulated NO signaling and VEGF-stimulated angiogenic responses (29). Moreover, TP508 is also effective in reversing ED-related effects of chronic myocardial ischemia (30) and acute myocardial infarct (31, 32). In injured tissues, TP508 has been shown to accelerate healing of dermal wounds (48–50), bone fractures (51) and segmental bone defects (52). All of these regenerative effects involve increased vascular recovery and stimulation of endothelial cells and progenitor stem cells (53–55). Therefore, we hypothesized that TP508 could mitigate radiation-induced damage to endothelial cells and increase survival after nuclear exposure.

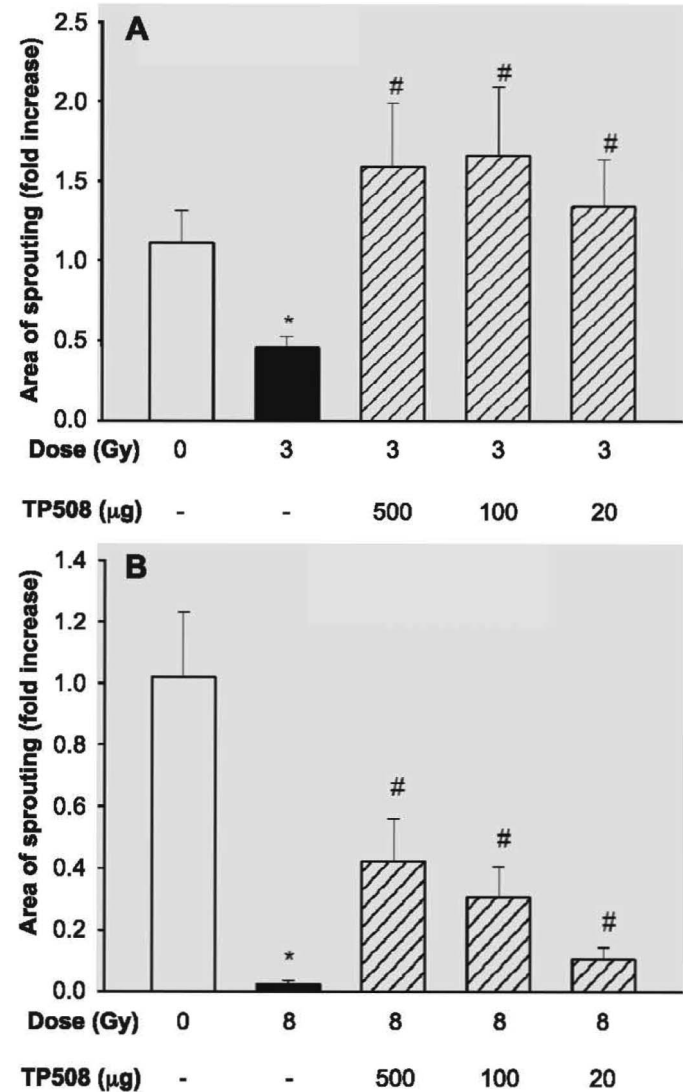


FIG. 6. Dose-dependent effect of TP508 on endothelial cell sprouting from aortic explants. Panel A: Thoracic aortas were isolated 24 h postirradiation from sham irradiated (open bars) or 3 Gy irradiated (black bar) CD-1 mice that were i.v. injected (tail vein) 1 h postirradiation with saline vehicle (black bar) or TP508 (hatched bars) at doses of 20, 100 or 500 µg per mouse. Aortic explants were cultured on Matrigel for 4 days and digital image areas of sprouting outgrowth were quantified. Data are expressed as a mean \pm SD, n = 6. * P < 0.05 compared to sham irradiation; # P < 0.05 compared with 3 Gy irradiation with saline. Panel B: Thoracic aortas were isolated 24 h postirradiation from sham- (open bars) or 8 Gy irradiated (black bar) CD-1 mice that were i.v. injected (tail vein) 1 h postirradiation with saline alone (black bar) or TP508 (hatched bars) at doses of 20, 100 or 500 µg per mouse. Data are expressed as a mean \pm SD, n = 6. * P < 0.05 compared to sham irradiation; # P < 0.05 compared to 8 Gy irradiation with saline alone.

Endothelial Cell Damage In Vitro

The current study demonstrated an 8 Gy dose of radiation significantly reduced VEGF-stimulated NO production in HCAEC 24 h postirradiation. However, stimulation of NO production by TP508 in these cells was still highly significant. Importantly, these studies also showed that if

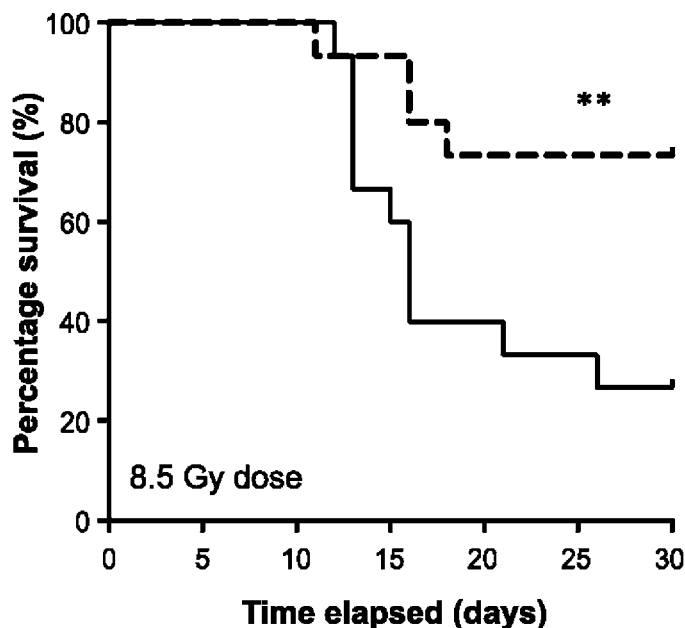


FIG. 7. Effect of TP508 on survival of CD-1 mice after whole-body gamma irradiation. Male 12-week-old CD-1 mice received 8.5 Gy irradiation, and at 24 h postirradiation injected (sc) with a single 100 μ l dose of sterile saline-alone (solid line) or sterile saline containing TP508 (350 μ g, 10 mg/kg; dashed line). The data are expressed based on Kaplan-Meier GraphPad analysis. $**P < 0.01$ compared to saline; $n = 20$ mice per group.

cells were treated with TP508 at 1 h postirradiation and then tested 24 h later, VEGF-stimulated NO production was partially restored. Furthermore, TP508 stimulated NO production in TP508-treated cells 1 h postirradiation was equivalent to that produced by TP508 stimulation of nonirradiated cells. Interestingly, Western blot analysis showed that radiation exposure caused a decrease in eNOS expression over this 24 h period. TP508 treatment 1 h postirradiation, however, attenuated the radiation-induced decrease in eNOS expression. Thus, the mitigating effect of TP508 on radiation-induced loss of NO signaling may be directly related to its maintenance of eNOS expression. In our prior studies, TP508 was shown to prevent hypoxia-induced down regulation of eNOS expression and to stimulate phosphorylation of eNOS through a mechanism that was distinct from that of VEGF (28). The current study is consistent with TP508 and VEGF having distinct effects on NO signaling and suggest that the mitigating effects of TP508 may reflect these mechanistic differences.

Previously published studies have shown that a dose of radiation (4 Gy) inhibited endothelial formation of tube-like angiogenic structures (56, 57). This current study shows that HDMEC also failed to form capillary-like interconnecting networks after irradiation (3 Gy). Interestingly however, if HDMEC are TP508 treated 1 h postirradiation and then tested 18 h later, tube formation is significantly increased compared to saline-alone-treated HDMEC. Tube formation *in vitro* is dependent on the angiogenic potential of the endothelial cells and their survival in the culture environ-

ment. These data therefore indicate that TP508 treatment mitigates radiation-induced effects and restores the angiogenic potential of endothelial cells.

To gain a better understanding of the mechanisms by which TP508 protects endothelial cells from the effects of ionizing radiation, we evaluated TP508 effects on repair of radiation-induced DNA damage in HDMEC. Ionizing radiation creates ROS inside of cells, resulting in DNA DSB which, if not repaired, drive cells toward senescence or apoptosis. Within seconds of DSB formation, histone H2AX is phosphorylated to form γ -H2AX that binds DSB to promote assembly of DNA repair enzyme complexes (40). Immunofluorescent staining of γ -H2AX therefore allows us to quantify DNA DSB in cells and determine if TP508 stimulates DNA repair to provide cellular protection from radiation. TP508 treatment of cells 1 h prior to 3 and 6 Gy irradiation accelerated DNA repair, resulting in a rapid decrease in the number of DSB visualized per cell and increased numbers of cells that had completely repaired DSB by 5 h. Interestingly, in other experiments (not shown) scrambled peptide with the same amino acid composition as TP508 but with scrambled sequence did not reduce the number of foci, suggesting that this effect of TP508 is specific for the TP508 peptide. Since unrepaired DSB lead to cell senescence and apoptosis, these results suggest that TP508 could, in fact, mitigate vascular damage caused by whole-body irradiation.

Endothelial Cell Damage In Vivo

Our understanding of radiation effects on endothelial cells has largely been generated through study of irradiated endothelial cells in culture. *In vivo* effects have largely been limited to histological examination of tissues from animals at various times after irradiation. For example, studies have shown early loss of microvascular endothelial cells in intestinal crypts preceding death of crypt stem cells (9). This early apoptosis of crypt endothelial cells, however, has been controversial and not seen by other investigators (58). We recently demonstrated that i.v. injection of TP508 stimulated changes in aortic endothelial cells (and/or endothelial progenitor cells) that resulted in significantly increased endothelial sprouting from aortic explants that were isolated from CD-1 mice 24 h after TP508 treatment (29). The aortic endothelial cell changes that were stimulated during the 24 h TP508 treatment *in vivo* in those experiments also enhanced sprouting induced by VEGF and prevented hypoxic inhibition of sprouting suggesting that this *ex vivo* assay could be used to test the effects of drugs on endothelial cell *in vivo* (29). Interestingly, it was recently reported that whole-body irradiation significantly reduced endothelial cell outgrowth from aortic explants using a similar assay (59). Thus, we used our aortic explant assay to determine if TP508 could reverse the loss of endothelial cell activity after whole-body irradiation.

Our current study showed that with as little as a 3 Gy dose of radiation, the aortic endothelial cell outgrowth from explants isolated 24 h postirradiation was reduced by approximately 50% and after a dose of 8 or 10 Gy, outgrowth was reduced by more than 95%. However, a TP508 treatment more than doubled the amount of endothelial outgrowth from sham-irradiated animal explants. More importantly, TP508 treatment significantly increased sprouting outgrowth in animal explants 1 h postirradiation (3, 8 and 10 Gy). In other experiments, animals were 3 or 8 Gy irradiated, and 1 h later received an injection of different doses of TP508. The animals that received 3 Gy irradiation showed maximal explant outgrowth with 100 and 500 μg TP508 treatment, but even with only 20 μg treatment, outgrowth was stimulated to levels exceeding the sham-irradiated group. Aortic explants taken from 8 Gy irradiated mice had less measurable outgrowth, but there was a clear dose response, with maximal outgrowth stimulated with 500 μg TP508 treatment, while 20 μg treatment had little effect.

With certain drugs there is not a good correlation between the dose that is efficacious in cultured cells and the dose required to be effective in animal cells or tissues. This can be due to the rapid degradation or clearance of systemically injected molecules compared to the continued stimulation caused by a drug that is left in tissue culture media for an extended period of time. It should be noted that as we moved from cultured endothelial cells to systemic injection, the effective doses appeared to be similar. That is, 50–200 $\mu\text{g}/\text{ml}$ TP508 treatment showed efficacy in endothelial cell cultures, and systemic injection of 100–500 μg per mouse appeared to be most effective in stimulating endothelial sprouting from aortic explants. Since a mouse has approximately 2 ml of blood, these doses are roughly equivalent. Furthermore, pharmacokinetic studies have demonstrated that the plasma half-life of TP508 is less than 20 min (53). Interestingly, we have also shown that up to 80% of TP508 is degraded or oxidized to form a peptide dimer during the first 90 min of incubation in endothelial cell tissue culture media. Thus, even in experiments where the media was not changed for 24 h, the duration of cell exposure to active monomeric TP508 would perhaps be similar to the duration of exposure expected after systemic injection in animals.

Another question that comes up in considering animal dosing is the route of drug delivery. For survival experiments that include large numbers of mice, sc injection is preferred to i.v. injection through the tail vein. Moreover, for emergency countermeasure use requiring field drug delivery to large numbers of people, sc injection is clearly preferred. We therefore conducted pharmacokinetic studies comparing i.v. and sc injections of TP508 in mice. The current study showed that with sc injection, the plasma concentration reaches a maximum at about 30 min after injection and then begins to gradually decline indicating slower adsorption into the blood, but due to a depot effect

the bioavailability is prolonged. Interestingly, the plasma concentration with sc injection at 30 min is roughly equivalent to that remaining at 30 min after i.v. injection. Thus, we chose to use a TP508 sc injection dose that was equivalent to the effective doses used in sprouting assays where i.v. injections were utilized.

Based on the endothelial outgrowth response seen with systemic injection of TP508, we performed experiments to determine whether these same concentrations of TP508 could mitigate lethal effects of nuclear radiation. In these experiments, we exposed male CD-1 mice to radiation doses that caused LD₇₀ in preliminary experiments. The results showed that a single injection of TP508 (350 μg per animal, sc, 10 mg/kg) administered 24 h postirradiation (8.5 Gy) increased the percentage of animals that survived for 30 days by more than 45% over saline-alone treated animals ($P < 0.01$). Similarly, in 9 Gy irradiated animals, a single TP508 treatment (10 mg/kg) increased survival by 38% over saline-alone treated animals (not shown). Thus, the effective dose of TP508 that stimulates aortic explant outgrowth is in the same range as the dose of TP508 that significantly increases survival. This raises the possibility that much of the increased survival may be mediated through TP508 activation or protection of endothelial cells in tissues and microvascular endothelial cells within stem cell niches.

We recently reported that TP508 treatment protected gastrointestinal crypts and stimulated proliferation of stem cells within crypts to maintain integrity of crypts and the gastrointestinal barrier (41). Consistent with our current study, the prior GI study used a single 24 h postirradiation TP508 injection of 500 μg (12.5 mg/kg). These studies also showed that protection of the intestinal crypts translated into significantly increased survival. We therefore hypothesize that the increased animal survival stimulated by TP508 in our current study, the TP508 maintenance of crypt integrity and activation of crypt stem cells (41) and the TP508 stimulation of endothelial cell sprouting from aortic explants after whole-body irradiation are all related to TP508 effects on endothelial cells. Mechanistically, based on our current results, it appears that TP508 mitigation of radiation-induced endothelial cell damage may involve TP508-induced acceleration of DNA DSB repair and restoration of NO signaling to restore endothelial function. Additional studies, however, are needed to understand the relationship between microvascular endothelial cell function, repair of irradiated tissues and survival after radiation exposure, as well as how TP508 mitigation of radiation-induced endothelial damage within the first 24 h relates to later effects on bone marrow stem cells and gastrointestinal crypts to increase survival.

ACKNOWLEDGMENTS

The authors would like to thank Dr. Bradford Loucas of the Department of Radiation Oncology at UTMB for assistance in irradiation of cell

cultures and mice used for these studies. This project is supported by NIH/NIAMD, grant no. 5R44AI086135. Chrysalis BioTherapeutics has licensed worldwide exclusive rights to TP508 (Chrysalin®) from The University of Texas Medical Branch. DHC and other employees receive compensation from Chrysalis BioTherapeutics and have stock or stock options in the company. Potential conflicts of interest are managed by the University of Texas Medical Branch Conflicts of Interest and Commitment Committee.

Received: February 8, 2016; accepted: May 31, 2016; published online: July 7, 2016

REFERENCES

- Messerschmidt O. Combined effects of radiation and trauma. *Adv Space Res* 1989; 9:197–201.
- DiCarlo AL, Maher C, Hick JL, Hanfling D, Dainiak N, Chao N, et al. Radiation injury after a nuclear detonation: medical consequences and the need for scarce resources allocation. *Disaster Med Public Health Prep* 2011; 5:S32–44.
- Chua HL, Plett PA, Sampson CH, Joshi M, Tabbey R, Katz BP, et al. Long-term hematopoietic stem cell damage in a murine model of the hematopoietic syndrome of the acute radiation syndrome. *Health Phys* 2012; 103:356–66.
- Cho YR, Lim JH, Kim MY, Kim TW, Hong BY, Kim YS, et al. Therapeutic effects of fenofibrate on diabetic peripheral neuropathy by improving endothelial and neural survival in db/db mice. *PLoS One* 2014; 9:e83204.
- Singh VK, Newman VL, Romaine PL, Wise SY, Seed TM. Radiation countermeasure agents: an update (2011–2014). *Expert Opin Ther Pat* 2014; 24:1229–55.
- Lyubimova N, Hopewell JW. Experimental evidence to support the hypothesis that damage to vascular endothelium plays the primary role in the development of late radiation-induced CNS injury. *Br J Radiol* 2004; 77:488–92.
- Krigsfeld GS, Savage AR, Billings PC, Lin L, Kennedy AR. Evidence for radiation-induced disseminated intravascular coagulation as a major cause of radiation-induced death in ferrets. *Int J Radiat Oncol Biol Phys* 2014; 88:940–6.
- Ahmed F, Ings SJ, Pizzey AR, Blundell MP, Thrasher AJ, Ye HT, et al. Impaired bone marrow homing of cytokine-activated CD34+ cells in the NOD/SCID model. *Blood* 2004; 103:2079–87.
- Paris F, Fuks Z, Kang A, Capodiceci P, Juan G, Ehleiter D, Haimovitz-Friedman A, et al. Endothelial apoptosis as the primary lesion initiating intestinal radiation damage in mice. *Science* 2001; 293:293–7.
- Suvorova T, Luksha LS, Lobanok LM. The effects of acute and chronic radiation on endothelium- and no-dependent vascular reactivity. *Cell Mol Biol (Noisy-le-grand)* 2005; 51:321–7.
- Gaugler MH, Neunlist M, Bonnaud S, Aubert P, Benderitter M, Paris F. Intestinal epithelial cell dysfunction is mediated by an endothelial-specific radiation-induced bystander effect. *Radiat Res* 2007; 167:185–93.
- Gaugler MH. A unifying system: does the vascular endothelium have a role to play in multi-organ failure following radiation exposure? *Br J Radiol* 2005; Supplement 27:100–5.
- Hatoum OA, Otterson MF, Kopelman D, Miura H, Sukhotnik I, Larsen BT, et al. Radiation induces endothelial dysfunction in murine intestinal arterioles via enhanced production of reactive oxygen species. *Arterioscler Thromb Vasc Biol* 2006; 26:287–94.
- McQuillan LP, Leung GK, Marsden PA, Kostyk SK, Kourambanas S. Hypoxia inhibits expression of eNOS via transcriptional and posttranscriptional mechanisms. *Am J Physiol* 1994; 267:H1921–7.
- Albina JE, Henry WL Jr., Mastrofrancesco B, Martin BA, Reichner JS. Macrophage activation by culture in an anoxic environment. *J Immunol* 1995; 155:4391–6.
- Anderson HD, Rahmutula D, Gardner DG. Tumor necrosis factor- α inhibits endothelial nitric-oxide synthase gene promoter activity in bovine aortic endothelial cells. *J Biol Chem* 2004; 279:963–9.
- Gao X, Xu X, Belmadani S, Park Y, Tang Z, Feldman AM, et al. TNF- α contributes to endothelial dysfunction by upregulating arginase in ischemia/reperfusion injury. *Arterioscler Thromb Vasc Biol* 2007; 27:1269–75.
- Horowitz S, Binion DG, Nelson VM, Kanaa Y, Javadi P, Lazarova Z, et al. Increased arginase activity and endothelial dysfunction in human inflammatory bowel disease. *Am J Physiol Gastrointest Liver Physiol* 2007; 292:G1323–36.
- Sugihara T, Hattori Y, Yamamoto Y, Qi F, Ichikawa R, Sato A, et al. Preferential impairment of nitric oxide-mediated endothelium-dependent relaxation in human cervical arteries after irradiation. *Circulation* 1999; 100:635–41.
- Getz GS, Reardon CA. Arginine/arginase NO NO NO. *Arterioscler Thromb Vasc Biol* 2006; 26:237–9.
- Predescu D, Predescu S, Shimizu J, Miyawaki-Shimizu K, Malik AB. Constitutive eNOS-derived nitric oxide is a determinant of endothelial junctional integrity. *Am J Physiol* 2005; 289:L371–81.
- Bateman RM, Sharpe MD, Ellis CG. Bench-to-bedside review: microvascular dysfunction in sepsis—hemodynamics, oxygen transport, and nitric oxide. *Crit Care* 2003; 7:359–73.
- Wang J, Zheng H, Ou X, Fink LM, Hauer-Jensen M. Deficiency of microvascular thrombomodulin and up-regulation of protease-activated receptor-1 in irradiated rat intestine: possible link between endothelial dysfunction and chronic radiation fibrosis. *Am J Pathol* 2002; 160:2063–72.
- Shi J, Wang J, Zheng H, Ling W, Joseph J, Li D, et al. Statins increase thrombomodulin expression and function in human endothelial cells by a nitric oxide-dependent mechanism and counteract tumor necrosis factor α -induced thrombomodulin downregulation. *Blood Coagul Fibrinolysis* 2003; 14:575–85.
- Hauer-Jensen M, Fink LM, Wang J. Radiation injury and the protein C pathway. *Crit Care Med* 2004; 32:S325–30.
- Wang J, Boerma M, Fu Q, Hauer-Jensen M. Significance of endothelial dysfunction in the pathogenesis of early and delayed radiation enteropathy. *World J Gastroenterol* 2007; 13:3047–55.
- Shires GT, Fisher O, Murphy P, Williams S, Barber A, Johnson G, et al. Recombinant activated protein C induces dose-dependent changes in inflammatory mediators, tissue damage, and apoptosis in in vivo rat model of sepsis. *Surg Infect* 2007; 8:377–86.
- Olszewska-Pazdrak B, Hart-Vantassell A, Carney DH. Thrombin peptide TP508 stimulates rapid nitric oxide production in human endothelial cells. *J Vasc Res* 2010; 47:203–13.
- Olszewska-Pazdrak B, Carney DH. Systemic administration of thrombin peptide TP508 enhances VEGF-stimulated angiogenesis and attenuates effects of chronic hypoxia. *J Vasc Res* 2013; 50:186–96.
- Fossum TW, Olszewska-Pazdrak B, Mertens MM, Makarski LA, Miller MW, Hein TW, et al. TP508 (Chrysalin) reverses endothelial dysfunction and increases perfusion and myocardial function in hearts with chronic ischemia. *J Cardiovasc Pharmacol Ther* 2008; 13:214–25.
- Osipov RM, Bianchi C, Clements RT, Feng J, Liu Y, Xu SH, et al. Thrombin fragment (TP508) decreases myocardial infarction and apoptosis after ischemia reperfusion injury. *Ann Thorac Surg* 2009; 87:786–93.
- Osipov RM, Robich MP, Feng J, Clements RT, Liu Y, Glazer HP, et al. The effect of thrombin fragment (TP508) on myocardial ischemia reperfusion injury in hypercholesterolemic pigs. *J Appl Physiol* 2009; 106:1993–2001.
- Carpenter AE, Jones TR, Lamproch MR, Clarke C, Kang IH, Friman O, et al. CellProfiler: image analysis software for identifying and quantifying cell phenotypes. *Genome Biol* 2006; 7:R100.
- Masson VV, Devy L, Grignet-Debrus C, Bernt S, Bajou K, Blacher S, et al. Mouse aortic ring assay: a new approach of the

- molecular genetics of angiogenesis. *Biol Proced Online* 2002; 4:24–31.
35. Lu J, Zhang K, Nam S, Anderson RA, Jove R, Wen W. Novel angiogenesis inhibitory activity in cinnamon extract blocks VEGFR2 kinase and downstream signaling. *Carcinogenesis* 2010; 31:481–8.
 36. Arnaoutova I, Kleinman HK. In vitro angiogenesis: endothelial cell tube formation on gelled basement membrane extract. *Nat Prot* 2010; 5:628–35.
 37. Gerhardt H, Betsholtz C. Endothelial-pericyte interactions in angiogenesis. *Cell Tissue Res* 2003; 314:15–23.
 38. Hamilton NB, Attwell D, Hall CN. Pericyte-mediated regulation of capillary diameter: a component of neurovascular coupling in health and disease. *Front Neuroenergetics* 2010; 2.
 39. Mahaney BL, Meek K, Lees-Miller SP. Repair of ionizing radiation-induced DNA double-strand breaks by non-homologous end-joining. *Biochem J* 2009; 417:639–50.
 40. Burma S, Chen BP, Murphy M, Kurimasa A, Chen DJ. ATM phosphorylates histone H2AX in response to DNA double-strand breaks. *J Biol Chem* 2001; 276:42462–7.
 41. Kantara C, Moya SM, Houchen CW, Umar S, Ullrich RL, Singh P, et al. Novel regenerative peptide TP508 mitigates radiation-induced gastrointestinal damage by activating stem cells and preserving crypt integrity. *Lab Invest* 2015; 95:1222–33.
 42. Soloviev AI, Tishkin SM, Parshikov AV, Ivanova IV, Goncharov EV, Gurney AM. Mechanisms of endothelial dysfunction after ionized radiation: selective impairment of the nitric oxide component of endothelium-dependent vasodilation. *Br J Pharmacol* 2003; 138:837–44.
 43. Burrell K, Hill RP, Zadeh G. High-resolution in-vivo analysis of normal brain response to cranial irradiation. *PLoS One* 2012; 7:e38366.
 44. Dimitrievich GS, Fischer-Dzoga K, Griem ML. Radiosensitivity of vascular tissue. I. Differential radiosensitivity of capillaries: a quantitative in vivo study. *Radiat Res* 1984; 99:511–35.
 45. Marks LB, Yu X, Vujaskovic Z, Small W Jr., Folz R, Anscher MS. Radiation-induced lung injury. *Semin Radiat Oncol* 2003; 13:333–45.
 46. Qiu J, Li J, He TC. Endothelial cell damage induces a blood-alveolus barrier breakdown in the development of radiation-induced lung injury. *Asia Pac J Clin Oncol* 2011; 7:392–8.
 47. Stewart FA, Hoving S, Russell NS. Vascular damage as an underlying mechanism of cardiac and cerebral toxicity in irradiated cancer patients. *Radiat Res* 2010; 174:865–9.
 48. Carney DH, Mann R, Redin WR, Pernia SD, Berry D, Heggors JP, et al. Enhancement of incisional wound healing and neovascularization in normal rats by thrombin and synthetic thrombin receptor-activating peptides. *J Clin Invest* 1992; 89:1469–77.
 49. Stierberg J, Norfleet AM, Redin WR, Warner WS, Fritz RR, Carney DH. Acceleration of full-thickness wound healing in normal rats by the synthetic thrombin peptide, TP508. *Wound Repair Regen* 2000; 8:204–15.
 50. Norfleet AM, Huang Y, Sower LE, Redin WR, Fritz RR, Carney DH. Thrombin peptide TP508 accelerates closure of dermal excisions in animal tissue with surgically induced ischemia. *Wound Repair Regen* 2000; 8:517–29.
 51. Wang H, Li X, Tomin E, Doty SB, Lane JM, Carney DH, et al. Thrombin peptide (TP508) promotes fracture repair by up-regulating inflammatory mediators, early growth factors, and increasing angiogenesis. *J Orthop Res* 2005; 23:671–9.
 52. Sheller MR, Crowther RS, Kinney JH, Yang J, Di Jorio S, Breunig T, et al. Repair of rabbit segmental defects with the thrombin peptide, TP508. *J Orthop Res* 2004; 22:1094–9.
 53. Carney DH, Olszewska-Pazdrak B. Could rusalatide acetate be the future drug of choice for diabetic foot ulcers and fracture repair? *Expert Opin Pharmacother* 2008; 9:2717–26.
 54. Olszewska-Pazdrak B, Bergmann JS, Fuller GM, Carney DH. The role of thrombin and thrombin peptides in wound healing and tissue repair. In: Maragoudakis ME, Tsopanoglou NE, editors. *Thrombin physiology and disease*. New York: Springer; 2009. p. 115–32.
 55. Freyberg S, Song YH, Muehlberg F, Alt E. Thrombin peptide (TP508) promotes adipose tissue-derived stem cell proliferation via PI3 kinase/Akt pathway. *J Vasc Res* 2009; 46:98–102.
 56. Park MT, Oh ET, Song MJ, Lee H, Park HJ. Radio-sensitivities and angiogenic signaling pathways of irradiated normal endothelial cells derived from diverse human organs. *J Radiat Res* 2012; 53:570–80.
 57. Ahmad M, Khurana NR, Jaber JE. Ionizing radiation decreases capillary-like structure formation by endothelial cells in vitro. *Microvasc Res* 2007; 73:14–9.
 58. Schuller BW, Rogers AB, Cormier KS, Riley KJ, Binns PJ, Julius R, et al. No significant endothelial apoptosis in the radiation-induced gastrointestinal syndrome. *Int J Radiat Oncol Biol Phys* 2007; 68:205–10.
 59. Soucy KG, Attarzadeh DO, Ramachandran R, Soucy PA, Romer LH, Shoukas AA, et al. Single exposure to radiation produces early anti-angiogenic effects in mouse aorta. *Radiat Environ Biophys* 2010; 49:397–404.